Genes Critical for Muscle Development and Function in *Caenorhabditis elegans* Identified through Lethal Mutations

Benjamin D. Williams and Robert H. Waterston

Department of Genetics, Washington University School of Medicine, St. Louis, Missouri 63110

Abstract. By taking advantage of a lethal phenotype characteristic of *Caenorhabditis elegans* embryos that fail to move, we have identified 13 genes required for muscle assembly and function and discovered a new lethal class of alleles for three previously known muscle-affecting genes. By staining mutant embryos for myosin and actin we have recognized five distinct classes of genes: mutations in four genes disrupt the assembly of thick and thin filaments into the myofilament lattice as well as the polarized location of these components to the sarcolemma. Mutations in another three genes also disrupt thick and thin filament assembly, but allow proper polarization of lattice components based on the myosin heavy chain isoform that we analyzed. Another two classes of genes are defined by mutations with principal effects on thick or thin filament assembly into the lattice, but not both. The final class includes three genes in which mutations cause relatively minor defects in lattice assembly. Failure of certain mutants to stain with antibodies to specific muscle cell antigens suggest that two genes associated with severe disruptions of myofilament lattice assembly may code for components of the basement membrane and the sarcolemma that are concentrated where dense bodies (Z-line analogs) and M-lines attach to the cell membrane. Similar evidence suggests that one of the genes associated with mild effects on lattice assembly may code for tropomyosin. Many of the newly identified genes are likely to play critical roles in muscle development and function.

THROUGH the application of genetic dissection, over 20 genes affecting muscle have been identified in the nematode *Caenorhabditis elegans*, including structural genes for several myosin heavy chain isoforms, paramyosin, actin, and twitchin (for review see Waterston, 1988). For the most part, genetic screens have focused on adults that move abnormally and have altered muscle structure. Although the recessive class of mutations causing this phenotype is now near genetic saturation, mutations in several genes that code for known muscle components remain to be identified (Cummins and Anderson, 1988; Barstead et al., 1991; Waddle et al., 1993). Clearly, new approaches will be needed to identify mutations in these and perhaps additional muscle-affecting genes. Extending the genetic analysis of muscle could identify new muscle components, provide insight into myofilament lattice assembly, and help to decipher the genetic program that regulates muscle cell gene expression.

An alternative phenotype that might be exploited in genetic screens is suggested by the discovery of lethal mutations in the genes *myo-3* (Waterston, 1989), *deb-1* (Barstead and Waterston, 1991), and *unc-45* (Venolia and Waterston, 1990). *myo-3* and *deb-1* code for myosin heavy chain A (mhcA)[1] and vinculin, respectively, both components of body wall muscle. The *unc-45* gene product is currently unknown, but genetic evidence (Venolia and Waterston, 1990) suggests that it interacts with mhcA and with myosin heavy chain B, the major heavy chain isoform in body wall muscle. Targeted genetic screens carried out for each of these genes resulted in the recovery of lethal mutations with a similar, distinctive phenotype (Waterston, 1989; Barstead and Waterston, 1991; Venolia and Waterston, 1990). Development appears normal until mid-embryogenesis when mutant embryos fail to begin moving; they begin but then stop elongation, the process which converts the early ovoid-shaped embryo into a worm-shaped larva. The paralyzed misshapen larvae hatch, but are inviable. Embryonic paralysis is correlated with obvious defects in body wall muscle structure. In a limited preliminary genome-wide screen for mutants with this phenotype, we demonstrated the feasibility of such an approach. Two mutations were identified, and both proved to be in muscle-affecting genes (Waterston, 1989; Barstead and Waterston, 1991).

Here we report the results of a more extensive genome-wide screen for mutants with this characteristic lethal phenotype. Although insufficient to identify all the genes in the class, our analysis adds 13 more, bringing the total to 16.

Address all correspondence to Dr. Benjamin D. Williams, Washington University School of Medicine, Department of Genetics, Box 8232, 4566 Scott Avenue, St. Louis, MO 63110.

1. *Abbreviation used in this paper*: mhc A, myosin heavy chain A.

A subset of these genes were previously defined through viable muscle-affecting mutations, and the new mutations represent important new alleles. The majority of the genes are newly identified. Antibody staining of mutant embryos for muscle components suggest that many of the genes are critical for myofilament lattice assembly, while others have minor effects on assembly, and at least some of these appear to be involved in the mechanisms which regulate contraction. Among the former are genes coding for the extracellular matrix protein perlecan (Rogalski et al., 1993) and the membrane protein β-integrin (Gettner, S., C. Kenyon, L. Reichardt, J. Plenefisch, M. B. Buchner, and E. Hedgecock. 1992. *Mol. Biol. Cell.* 3:1088a), indicating the importance of the ECM and cell membrane in lattice assembly. Among the latter are genes which may code for tropomyosin and troponin C. The new mutations described here have provided new insights into muscle assembly, when combined with more detailed description of wild-type muscle development, as presented in the accompanying paper (Hresko et al., 1994).

Materials and Methods

General Methods and Strains

Methods for handling worms, including EMS mutagenesis, were as described by Brenner (1974) and in Sulston and Hodgkin (1988). The N2 wild-type strain of *C. elegans* var Bristol was the parental strain for all mutant screens. The BO wild-type strain var Bergerac, strain RW7000, was used in inter-strain crosses for some genetic mapping experiments as described (Williams et al., 1992). Other genes and mutations used in this study, all originally generated from N2 wild-type parents, are listed by chromosome: LG *I*, *unc-11(e41)*, *unc-38(x20)*, *dpy-5(e61)*, *unc-29(el072)*, *unc-13(e323)*, *unc-54(el213)*, *unc-87(e843)*, *unc-120(st364ts)*, *unc-94 (sul77)*, and *mec-8(e398)*; LG *II*, *tra-2(q122)*, and *unc-52(e669)*; LG *III*, *vab-6(e697)*, *unc-45(st601)*, *unc-45(e286ts)*, *daf-7(el372ts)*, *dpy-1(el)*, *unc-93(el500)*, *dpy-27(y57)*, *unc-79(el068)*, *dpy-17(el164)*, *dpy-19(el259)*, *unc-32(el89)*, *emb-9(hc70ts)*, and *unc-69(e587)*; LG *IV*, *dpy-9(el2)*, *unc-44(e362)*, *deb-1(st385)*, *unc-82(el323)*, *unc-5(e53)*, and *unc-24(el38)*; LG *V*, *dpy-11(e224)*, *unc-23(e25)*, *myo-3(e386)*, *sqt-3(e24)*, *unc-39(e257)*, and *unc-112(r367)*; LG *X*, *let-2(g30)* and *unc-3(el51)*.

The chromosome *X* duplications *mnDp1* and *mnDp8*, and deficiencies *mnDf1* and *mnDf8* were also used. Deficiencies *mnDf41*, *stDf7*, and *stDf8* were used to map mutations on chromosome *IV*.

Strains were obtained from the Waterston laboratory collection or the *Caenorhabditis* Genetics Center with the exceptions of a *tra-2(q122)* strain, a gift of T. Schedl, and the strains used to map *pat-3* (see Table I), which were gifts of J. Plenefisch.

Mutant Screens

N2 wild-type hermaphrodites were treated with 0.050 M EMS for 4 h, and then were allowed to reproduce on fresh plates. Individual F1 progeny were then placed on separate plates at 20°C, allowed to lay ~50 eggs, and then removed. The next day plates were checked by dissecting microscope and those in which 1/4 of the embryos had arrested at the twofold length, hatched or unhatched, were retained. Heterozygous strains were then established by picking phenotypically wild-type siblings.

Each twofold arrest mutant was examined for abnormal embryonic movements during mid-embryogenesis by time-lapse video, as follows: ~20 bean-stage embryos produced by a heterozygous parent were positioned in a tight grouping near the edge of a circular 2% agarose pad prepared in buffer A (50 mM NaCl, 10 mM Tris, pH 7.0) as described (Wood et al., 1988) with the following modifications. After a small drop of buffer A was added to the center of the pad, a square coverslip of slightly larger dimension was gently lowered in place, immobilizing the embryos. The coverslip

Table I. Three-Factor Crosses

Gene	Genotype of heterozygote	Summary of recombination events*
pat-10	*unc-11 + dpy-5/+ pat-10 +*	*unc-11* (12/16) *pat-10* (4/16) *dpy-5*
	unc-38 + dpy-5/+ pat-10 +	*unc-38* (2/14) *pat-10* (12/14) *dpy-5*
	+ dpy-5 unc-29/pat-10 + +	[*pat-10 dpy-5*] (15/15) *unc-29*
pat-11	*dpy-5 + unc13/ + pat-11 +*	*dpy-5* (10/47) *pat-11* (37/47) *unc-13*
pat-4	*+ unc-45 dpy-1/pat-4 + +*	[*pat-4 unc-45*] (54/54) *dpy-1*
	+ unc-45 daf-7/pat-4 + +‡	[*pat-4 unc-45*] (32/32) *daf-7*
	pat-4 + daf-7/+ unc-45 +§	*pat-4* (3/57) *unc-45* (54/57) *daf-7*
pat-12	*unc-45 + daf7/+ pat-12 +‡*	*unc-45* (17/30) *pat-12* (13/30) *daf-7*
pat-3	*unc-93 + dpy-17/+ pat-3 +*	*unc-93* (15/34) *pat-3* (19/34) *dpy-17*
	unc-93 dpy-27 +/+ + pat-3	*unc-93* (8/8) [*dpy-27 pat-3*]
	+ dpy-27 unc-79/pat-3 + +	[*pat-3 dpy-27*] (7/7) *unc-79*
pat-2	*dpy-19 + unc-32/+ pat-2 +*	*dpy-19* (24/28) *pat-2* (4/28) *unc-32*
emb-9	*dpy-19 + unc-69/+ emb-9 +*	*dpy-19* (4/14) *emb-9* (10/14) *unc-69*
pat-5	*unc-5 + dpy-24/+ pat-5 +*	*unc-5* (9/12) *pat-5* (3/12) *unc-24*
pat-8	*unc-5 + dpy-24/+ pat-8 +*	*unc-5* (11/17) *pat-8* (6/17) *unc-24*
unc-112	*dpy-11 unc-23 +/+ + unc-112*	*dpy-11* (16/16) [*unc-23 unc-112*]
	sqt-3 unc-39 +/+ + unc-112	*sqt-3* (8/8) [*unc-39 unc-112*]

* Data are presented in two forms: *a (l/t) b (r/t) c* and *a (t/t) [b c]*. The first indicates that in *t* recombination events between *a* and *c*, *l* were between *a* and *b*, and *r* were between *b* and *c*. This definitively establishes the gene order *a b c*. The ratios *l/t* and *r/t* reflect the relative genetic distances from *a* to *b* and *b* to *c*, respectively. The second form indicates that all *t* recombination events between *a* and *b* also occurred between *a* and *c*. Although this establishes that *a* is left of *b* and *c*, the relative positions of *b* and *c* with respect to each other cannot be determined from these data, as indicated by the brackets.

‡ Daf non-Unc recombinants were isolated to separate plates at 25°C, shifted to 15°C to reverse the Daf phenotype, allowed to self-fertilize, and the plates were then scored for the presence of 1/4 twofold arrest progeny.

§ Daf non-Pat recombinants were isolated to separate plates at 25°C, shifted to 15°C to reverse the Daf phenotype, and allowed to self-fertilize. After the resulting progeny had hatched, plates were shifted to 25°C (the restrictive temperature for the *unc-45* mutation) for 24 h and were then scored for the Unc phenotype.

was then sealed with silicone grease leaving two small gaps (~2 mm) at opposite sides. Additional buffer A was added through one gap to fill the chamber, but leaving an air/buffer interface close to the group of eggs. Using these conditions we found that embryos developed and eventually hatched without becoming anoxic, and that they remained in the same focal plane even though some water in the chamber evaporated during the period of observation. Embryos were observed using standard Nomarski optics, and time-lapse video recordings were made using a Toshiba KV-6110A VCR adjusted to an 18:1 time compression.

Genetic Mapping

The lethal Pat mutations were first mapped to a chromosome and sometimes to a chromosomal subregion using a rapid multi-factor mapping method that is based on the simultaneous detection of multiple polymorphisms by the PCR (Williams et al., 1992). The mapping data for *pat-9, deb-1,* and *myo-3* were published in the report describing this mapping method; the rest is not shown.

Three-factor analysis and duplications and deficiencies were used for more detailed mapping. The three-factor data were generated using standard techniques (Wood et al., 1988) and are presented in Table I.

The *X*-linked mutation *pat-9(st558)* was shown to be included in duplications *mnDp1* and *mnDp8* by the viability of hemizygous males with the genotypes *mnDp1/+ I; pat-9(st558)/0 X* and *mnDp8/+ V; pat-9(st558)/0 X*, respectively. These genotypes were verified by mating the males with N2 wild-type hermaphrodites and the recovery of *pat-9(st558)/+* hermaphrodite progeny. *mnDp8* is not a simple duplication, suggested by the fact that it fails to include *let-2*, but does include genes mapped to either side of this locus. Since *mnDp8* includes *pat-9(st558)*, *pat-9(st558)* does not appear to be an allele of *let-2*. This is further suggested by the complementation of *pat-9(st558)* and the conditional lethal *let-2(g30ts)* mutation, as shown by the wild-type phenotype of *pat-9(st558) +/+ let-2(g30ts)* hermaphrodites at the restrictive temperature (25°C). These animals were identified through their segregation of 1/2 wild-type and 1/2 twofold arrest progeny, and were constructed by crossing *mnDp1/+ I; pat-9(st558)/0 X* males with *let-2(g30ts)* hermaphrodites at the permissive temperature (15°C), brooding the fertilized hermaphrodites at 25°C, and then cloning wild-type progeny. If the *pat-9* and *let-2* mutations had failed to complement, wild-type animals of genotype *mnDp1/+ I; pat-9(st558)/g30ts X* might have been recovered using this procedure, but would have segregated only 1/4 twofold arrested progeny, the zygotes failing to inherit *mnDp1*.

The mutation *pat-9(st558)* was marked with *unc-3(e151)* in *cis* and mapped using deficiencies *mnDf1* and *mnDf8* as described (Meneely and Herman, 1979). *mnDf1* uncovers *pat-9*, and *mnDf8* does not. These results position *pat-9* in the interval defined by the right end points of *mnDf1* and *mnDf8*.

The deficiencies *nDf41*, *stDf7*, and *stDf8* on chromosome *IV* uncover *deb-1*, *pat-5*, and *pat-8*, as indicated by the appearance of twofold arrest progeny in separate crosses between the appropriate deficiency heterozygotes (hermaphrodites) and lethal heterozygotes (males). F1 deficiency homozygotes (produced by self-fertilization) arrested development during early embryogenesis, and were therefore easily distinguishable from the twofold arrest cross progeny. *unc-82* is also uncovered by these three deficiencies as demonstrated by the disorganized muscle phenotype (verified by polarized light microscopy) of *unc-82 unc-24/nDf41*, *unc-44 unc-82/stDf7*, and *unc-44 unc-82/stDf8* hermaphrodites, respectively.

Complementation Tests

For lethal mutation *a* and recessive non-lethal mutation *b*, failure to complement was indicated by phenotype B male progeny from *a/+* male and *b/b* hermaphrodite parents (male progeny were scored since they are produced in significant numbers only through fertilization by the male parent and not through self-fertilization of the hermaphrodite parent). If a test indicated complementation, the result was confirmed by the recovery of *a +/+ b* wild-type F1 hermaphrodites.

Complementation tests between lethal mutations *a* and *b* were carried out by crossing *a/+; tra-2(q122)/+* females (rendered incapable of self-fertilization by the *tra-2* mutation) with *b/+* males as described (Barstead and Waterston, 1991). Production of Pat progeny indicated failure of *a* and *b* to complement. When Pat progeny were not observed, complementation was confirmed by isolating a phenotypically wild-type hermaphrodite with genotype *a +/+ b* from the cross progeny. This same procedure was used to show that *emb-9(st540)* and *emb-9(hc70ts)* fail to complement, except that *tra-2(q122)/+; emb-9(hc70ts)/+* females were generated at the permissive temperature (15°C), and the complementation test was then performed at the restrictive temperature (25°C).

Pat mutations mapping near each other were tested for complementation. Representative alleles were then tested for complementation against mutations in previously identified muscle-affecting genes in the same region. Mutations were assigned to the same gene if they mapped near one another and failed to complement (see Results). Other complementation results are as follows: *pat-11(st541)* complements *unc-87(e843)*, *unc-120(st364ts)*, and *unc-94(su177)*. It also complements the touch-insensitive mutant *mec-8(e398)*. This test was done because double mutants with *mec-8* (touch-insensitive alleles) and *unc-52* (viable Unc alleles) have a synthetic Pat phenotype, raising the possibility that *mec-8* loss-of-function alleles might be Pat (Herman, R., personal communication). *pat-4(st559)* and *pat-12(st430)* complement both the temperature sensitive Unc mutation *unc-45(e286ts)* and the Pat mutation *unc-45(st601)*. *pat-4(st579)* complements *vab-6(e697)*. *pat-5(st556)*, *pat-8(st554)*, and *deb-1(st386)* each complement *unc-82(e1323)*.

The complementation test between *let-2(st550)*, isolated here, and the temperature sensitive *let-2(g30ts)* mutation was performed by crossing *let-2(st550)/+* hermaphrodites with *let-2(g30ts)/0* males at 15°C, the permissive temperature for *let-2(g30ts)*. Hermaphrodites with genotype *let-2(st550)/let-2(g30ts)* were recovered and are viable at the permissive temperature, as verified by allowing separate groups of eggs produced by self-fertilization to develop at 15°C and at 25°C, the restrictive temperature. The former produced 1/4 twofold arrest progeny (the *let-2(st550)* homozygotes) while the latter produced 100% twofold arrest progeny, indicating failure of *st550* and *g30ts* to complement.

Estimation of Gene Number

The number of severe Pat genes was estimated by the method of Meneely and Herman (1979), which uses the Poisson distribution to calculate the gene number from the fraction of genes represented by more than one mutant allele. The observed distribution of mutations per gene (excluding mutations identified in directed screens) does not, at least superficially, appear to be different than Poisson. The observed and expected (the latter calculated for a 13 gene class and shown in parenthesis) number of genes with 1, 2, 3, 4, and 5 alleles are: 2 (2.87), 3 (3.18), 3 (2.86), 2 (1.92), and 2 (1.03), respectively, which gives a χ^2 value having a probability between 0.7 and 0.9. Since there are only a small number of genes in each class, the reliability of χ^2 analysis is questionable, however.

Antibody Staining

Populations of embryos from heterozygous parents were fixed and stained, and mutant homozygotes were distinguished from their phenotypically wild-type siblings either by their characteristic abnormal muscle morphology (one-and-three-quarters-fold embryos stained with DM5.6) or their distorted body shapes (post-elongation-arrest embryos). For staining of *pat-3* and *lev-11* mutants with monoclonal antibody MH25 and anti-tropomyosin, respectively, all post-elongation-arrest embryos, easily recognized by their distorted shapes, failed to stain or had greatly reduced staining. Approximately 1/4 of the pre-elongation arrest embryos failed to stain, as expected. Methods for fixing and staining the embryos were as described (Barstead and Waterston, 1991). Briefly, eggs were released from gravid adults by hypochlorite treatment, and then fixed with buffered 3% formaldehyde at room temperature followed by methanol at −20°C. Monoclonal antibodies DM5.6 (Miller et al., 1983), MH27 (Francis and Waterston, 1991), C4 (Chemicon International, Inc., Temecula, CA), and MH25 (Francis and Waterston, 1985) were used at dilutions of 1:1,500, 1:1,000, 1:100 and 1:200, respectively, with fluorescein-labeled goat anti-mouse (Chemicon International, Inc.) at dilution 1:100 serving as a secondary antibody. The affinity purified anti-tropomyosin, generated in rabbits, was a generous gift of M. Hresko and L. Schriefer. The rabbit polyclonal anti-myosin (Francis, G. R., and R. H. Waterston, unpublished observations) was used at dilution 1:750. Rhodamine-labeled goat anti-rabbit (Chemicon International, Inc.) diluted 1:100 was the secondary antibody used with both of the primary rabbit antisera. Photographic exposures were made on T-Max 400 film which was then processed according to instructions.

Results

The Pat Mutant Phenotype

We refer to the lethal phenotype of the *myo-3*, *deb-1*, and *unc-45* mutants as Pat for paralyzed, arrested elongation at twofold. Wild-type embryos (Fig. 1 *a*) start to lengthen into a

worm shape mid-way through embryogenesis, and soon after they reach the one-and-one-half-fold length, begin to move, just as the myofilament lattice within the body wall muscle cells is becoming well organized (Hresko et al., 1994). Initially the embryos twitch weakly, but within a few minutes, by the twofold stage, they are rolling vigorously within the egg. In contrast, Pat mutants (Fig. 1 *b*) do not start moving at the normal time and remain paralyzed as elongation continues. At the twofold stage, elongation arrests. Development continues, however, as indicated by cuticle formation and development of a well-formed pharynx. The myofilament lattice in body wall muscle cells is abnormal.

Screen for Pat Mutants

Wild-type hermaphrodite parents were mutagenized and then F1 animals produced by self-fertilization were cloned to separate plates and allowed to lay eggs. By using 24-h broods, eggs arrested at twofold or twofold larvae were readily recognized using the 50 × objective of a dissecting microscope. We did not require the arrested embryos to hatch, since pharyngeal pumping appears to aid hatching and we did not want to exclude mutants with defective pharyngeal muscles. In a final screening step we observed the movements of each of the twofold arrest mutants during mid-embryogenesis using Nomarski microscopy in combination with video time-lapse.

About half of the isolates were severely paralyzed ("severe" Pat phenotype) and further work concentrates on this group. The others fell into two classes. The "mild" Pat mutants began twitching movements at one-and-one-half-fold, and continued to twitch for several hours. These mutants never exhibited the vigorous rolling movements seen in wild-type embryos by the twofold stage. The second class had the Lat phenotype (late paralysis, arrested elongation at twofold). These animals began twitching at one-and-one-half-fold and by twofold were rolling as well as similarly staged wild-type embryos; movement and elongation stopped nearly simultaneously soon after the twofold stage.

From a screen of 2900 F1 clones, 33 severe Pat mutants were isolated. These are listed along with severe Pat mutants *deb-1(st385)* and *myo-3(st386)*, isolated in a previous unrestricted screen of 500 F1 clones (Waterston, 1989), and *pat-8(st554)* and *pat-5(st556)*, recovered in a screen directed to the genetic interval near *unc-44* on chromosome *IV* (Barstead and Waterston, 1991).

From the same screens, we also selected two mild Pat and three Lat mutants since these phenotypes could also be consistent with a defect in muscle. Indeed, the previously described *unc-45* mutants have the mild Pat phenotype when their parent contains a wild-type allele (e.g., genotype *unc-45(st601)/+*) (our unpublished observations; Venolia and Waterston, 1991), apparently due to a partial maternal rescue.

Genetic Mapping and Complementation Tests

The results of genetic mapping and complementation analysis (see Materials and Methods) are summarized in Table II which lists the 15 Pat genes examined here and their corresponding mutant alleles, and Fig. 2, which shows the locations of all 16 currently identified Pat genes on the genetic map (indicated above each chromosome). No new alleles of *unc-45* were recovered in this study, perhaps because we only analyzed two mutants with the mild Pat phenotype. Ten of the genes appear to be newly identified and have been named *pat-2* through *pat-6*, and *pat-8* through *pat-12*. Five, *myo-3*, *deb-1*, *unc-52*, *unc-112*, and *lev-11* are previously defined muscle-affecting genes. Of the previously identified genes, only *myo-3* and *deb-1* have been associated with the Pat phenotype before. *unc-52* and *unc-112* were originally identified through Unc mutants with progressive

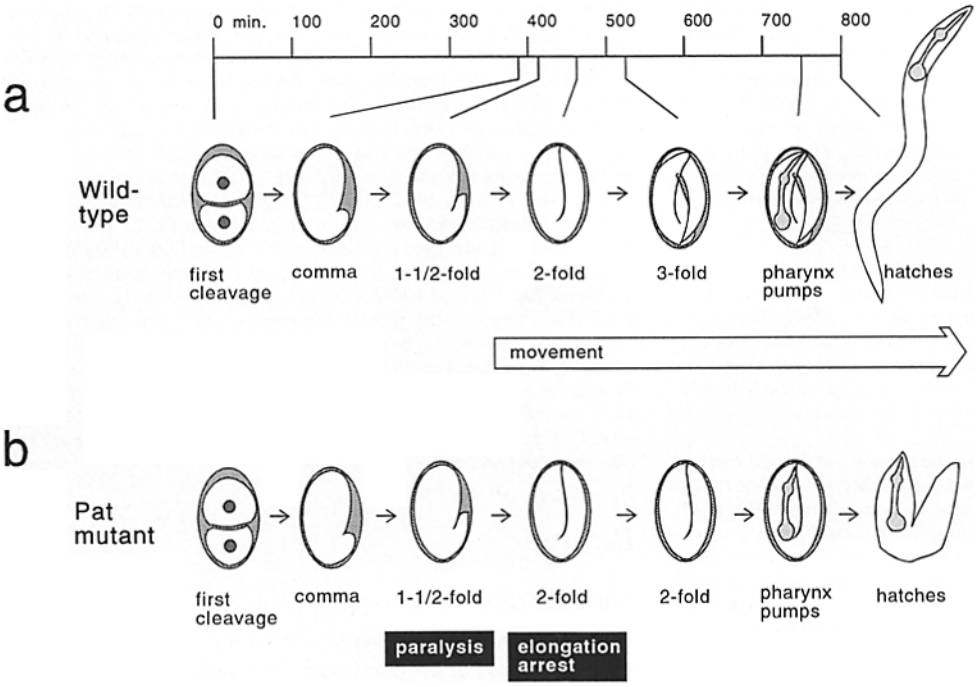

Figure 1. Embryogenesis in wild-type and Pat mutants. (*a*) Wild-type; the first contractions of body wall muscles occur as the embryos reach the one-and-one-half-fold length. By twofold, embryos roll vigorously within the egg (diagram adapted from Sulston et al. [1983]). (*b*) Pat mutants; one-and-one-half-fold embryos fail to start moving, and remain severely paralyzed. Elongation continues until the embryos are twofold, but then stops. Pharyngeal morphogenesis occurs and embryos often hatch near the normal time as misshapen, inviable larvae.

Table II. Genetic Loci and Corresponding Mutations

Gene	Chromosome	Mutation
Severe paralysis		
myo-3	*V*	*st386**‡, *st563*‡, *st565*‡
deb-1	*IV*	*st385**‡, *st555*§‡
unc-52	*II*	*st546*, *st549*‡, *st560*, *st572*, *st578*
unc-112	*V*	*st562*‡, *st581*
lev-11	*I*	*st536*, *st557*‡, *st566*‡
pat-2	*III*	*st538*‡, *st543*, *st422*, *st567*‡
pat-3	*III*	*st423*, *st552*, *st564*‡
pat-4	*III*	*st551*, *st559*‡, *st579*‡, *st580*
pat-5	*IV*	*st553*, *st556*§, *st569*, *st571*‡, *st576*, *st577*‡
pat-6	*IV*	*st561*, *st570*‡
pat-8	*IV*	*st554*§‡
pat-9	*X*	*st558*‡
pat-10	*I*	*st568*‡, *st575*‡
Mild paralysis		
pat-11	*I*	*st541*‖
pat-12	*III*	*st430*‡
Late paralysis		
emb-9	*III*	*st540*‖, *st545*
let-2	*X*	*st550*‖

* Isolated in previously reported unrestricted screen (Waterston, 1989).
‡ Pharyngeal pumping movements observed in some of the mutant homozygotes.
§ Isolated in a screen for Pat mutants linked to *unc-44* (Barstead and Waterston, 1991).
‖ Pharyngeal muscles appear paralyzed in all of the mutant homozygotes that we observed.

muscular dysfunction (Brenner, 1974; Bejsovec, A., and P. Anderson, personal communication; Francis, G. R., and R. H. Waterston, unpublished results). The *unc-52* gene has recently been shown to code for the *C. elegans* homolog of perlecan, a proteoglycan component of the extracellular matrix (Rogalski et al., 1993). *lev-11* was identified through mutants selected for their resistance to the acetylcholine agonist levamisole (Lewis et al., 1980), which causes wild-type worms to hyper-contract their body wall muscles. In the absence of the drug these mutants locomote normally, but show incessant subcellular twitching within their body wall muscle cells.

The Lat mutations were found to be alleles of either *emb-9* or *let-2* (Table II and Fig. 2, *boxes*), genes originally defined by temperature sensitive lethal mutations (Miwa et al., 1980; Meneely and Herman, 1979), and known to code for collagen type IV, a component of basement membranes (Guo et al., 1991; Sibley et al., 1993).

For genes with more than one corresponding mutant, we observed no differences between mutants in their embryonic movements. Although we did not characterize the muscle assembly defects of all the mutants by antibody staining (see below), in instances where we analyzed more than one allele of a particular gene, each caused the same phenotype, with one exception (see below). These observations, the mutation frequency for the genes with multiple mutant alleles as well as the failure of *pat-3*, *lev-11* (see below) and *unc-52* (Rogalski et al., 1993) Pat mutants to stain with antibodies to their putative gene products, suggest that many of the mutations result in gene loss-of-function. It should be pointed out, however, that the natures of the mutations have not yet been determined. Consequently, our interpretations of gene product function based on the analysis of the mutant muscle assembly (see below) are subject to the caveat that in some instances the mutant phenotypes may be caused by the interference of an abnormal gene product, rather than the simple absence of a functional product.

Pharyngeal Muscles

The pharynx is the second largest muscle in *C. elegans* and normally begins pumping movements approximately 1 h before the embryos hatch. Although different myosin heavy chain genes are expressed in body wall and pharyngeal muscle cells (Epstein et al., 1974; Waterston et al., 1982; Ardizzi and Epstein, 1987), at least a subset of other muscle component genes appear to be coexpressed in these two muscle types (Waterston et al., 1980, 1984; Ardizzi and Epstein, 1987; Francis, G. R., and R. H. Waterston, unpublished results). Consequently, some of the Pat mutants might be expected to have pharyngeal defects. Our time-lapse video analysis was usually limited to mid-embryogenesis, but sometimes observations were extended through hatching, and in favorable instances we could score for pharyngeal movement. Although we have not analyzed the pharyngeal phenotype carefully, the *pat-11* mutant never pumped, in contrast to the other Pat genes where one or more mutants did pump (Table II, footnotes). Our limited observations suggest that there may be variability between the Pat mutants in the percentage of animals that can pump, and in the vigor of pumping. In individuals that failed to pump, we observed no obvious defects in pharyngeal structure and shape other than those apparently related to the body elongation defect. We did not, however, examine the structure of the pharyngeal muscle cells in detail. Further analysis of the pharyngeal phenotype may be informative.

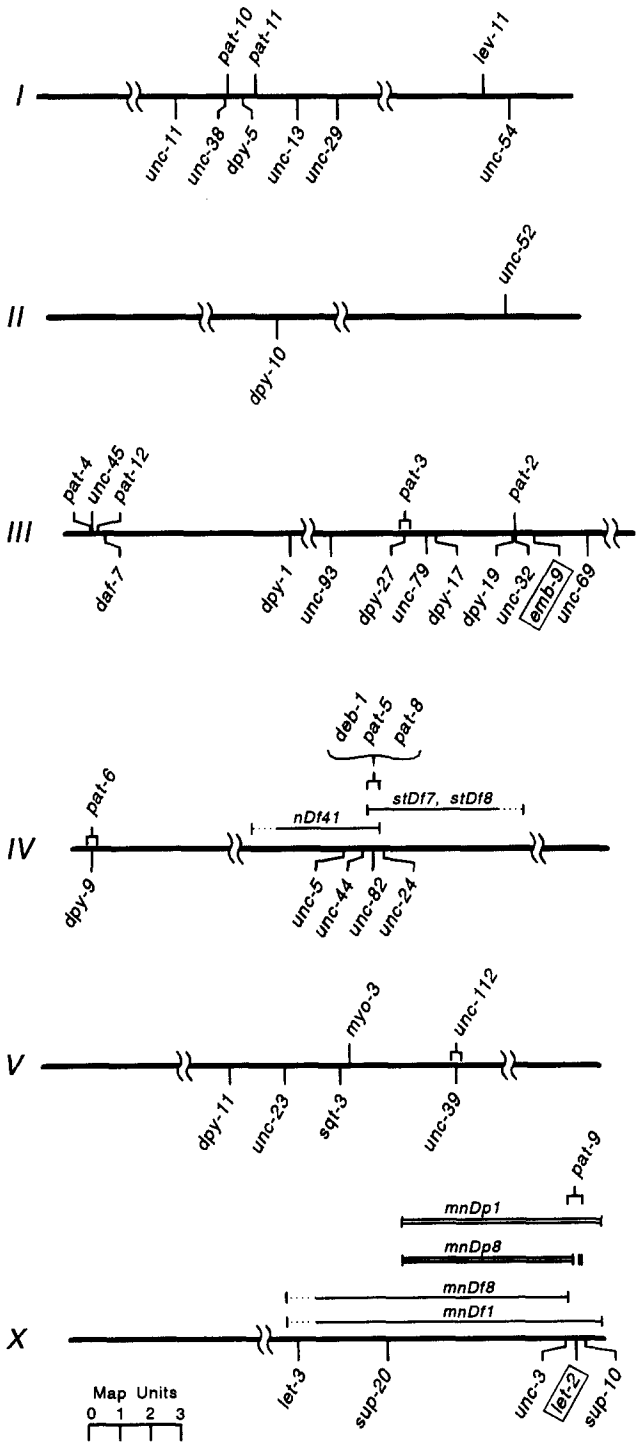

Figure 2. Genetic map positions of genes associated with the Pat phenotype. Pat genes are shown above each chromosome; genes used in genetic mapping experiments, and those associated with the Lat phenotype (in boxes), are shown below. In instances where the current mapping data fail to position a Pat gene relative to a marker, its position is indicated with a bracket. The extent of deficiencies (*single lines*) and duplications (*double lines*) used in mapping are indicated above chromosomes *IV* and *X*. *deb-1*, *pat-5*, *pat-8*, and *unc-82* are uncovered by deficiencies *mnDf41*, *stDf7* and *stDf8*, placing these genes in the interval where the deficiencies overlap. *pat-9* is uncovered by *mnDf1*, but not by *mnDf8*, placing it somewhere in the interval defined by the right endpoints of these two deficiencies. *pat-9* is included in the duplications *mnDp1* and *mnDp8*. The gap in the latter indicates that it fails to include *let-2* but does include some markers to the right of this gene (see Materials and Methods for details).

It is noteworthy that during the culture of *pat-11* mutant strains most mutant embryos did not hatch. A similar though apparently less severe defect in hatching was observed for the *pat-5* and *lev-11* mutants, suggesting compromised pharyngeal function. All of the *emb-9* and *let-2* mutants that we observed did not pump, and in culture most of these mutant embryos either failed in hatching or were greatly delayed.

Pat Embryos Stained with Anti-Myosin

To learn more about the effects of the Pat mutations on body wall muscle development, we assessed the assembly state of the two major filament systems within the myofilament lattice by staining the embryos with monoclonal antibodies recognizing mhcA and actin. To readily place the body wall muscle cells in the context of the embryo, we often included a monoclonal antibody that stains the adherens junctions between hypodermal cells. These thin cells form the outer surface of the embryo and change shape dramatically during embryonic elongation (Priess and Hirsh, 1986). Embryonic length and hypodermal cell shape were used to accurately determine the age of pre-elongation-arrest embryos in the unsynchronized populations that we stained.

For mhcA staining, one-and-three-quarters-fold embryos were compared since this is the stage when mhcA first appears well-organized in wild-type embryos (see below). The arrangement of body wall muscle in wild-type embryos at this stage is shown diagrammatically in Fig. 3. Body wall muscle runs longitudinally in two dorsal and two ventral strips, or quadrants, just beneath the hypodermal cells. Each quadrant is a double row of overlapping spindle-shaped muscle cells. By hatching, these cells are attached to the hypodermis, and are polarized in the sense that the myofilament lattice is positioned asymmetrically within the cell, subtending the membrane in contact with the hypodermis. In the one-and-three-quarters-fold embryo, lattice components are already accumulating near the sarcolemma and the lattice is partially assembled at this position. Attachments between the muscle cells and the hypodermis are also forming at this stage. These events are described in detail in the accompanying paper (Hresko et al., 1994). Fig. 3 *a* diagrams the left dorsal surface of an embryo showing the arrangements of muscle cells within a dorsal muscle quadrant as well as the outlines of the hypodermal cells. Greater detail is shown in Fig. 3 *b*, including the position of the two myosin-containing A-bands that are forming within each muscle cell; this number of A-bands is maintained through hatching. The A-bands are semi-longitudinal due to the staggered position of laterally adjacent contractile units, a characteristic of *C. elegans* obliquely striated muscle (for a diagram of adult myofilament lattice structure see Fig. 2 of Francis and Waterston [1985]). One landmark for the dorsal quadrant is the circular junction between four hypodermal cells at the position of a developing sensillum called the deirid (Fig. 3 *b*).

A comparable view of a wild-type embryo double-stained with anti-mhcA and the antibody to hypodermal cell junctions is shown in Fig. 4 *b*. MhcA is organized into two

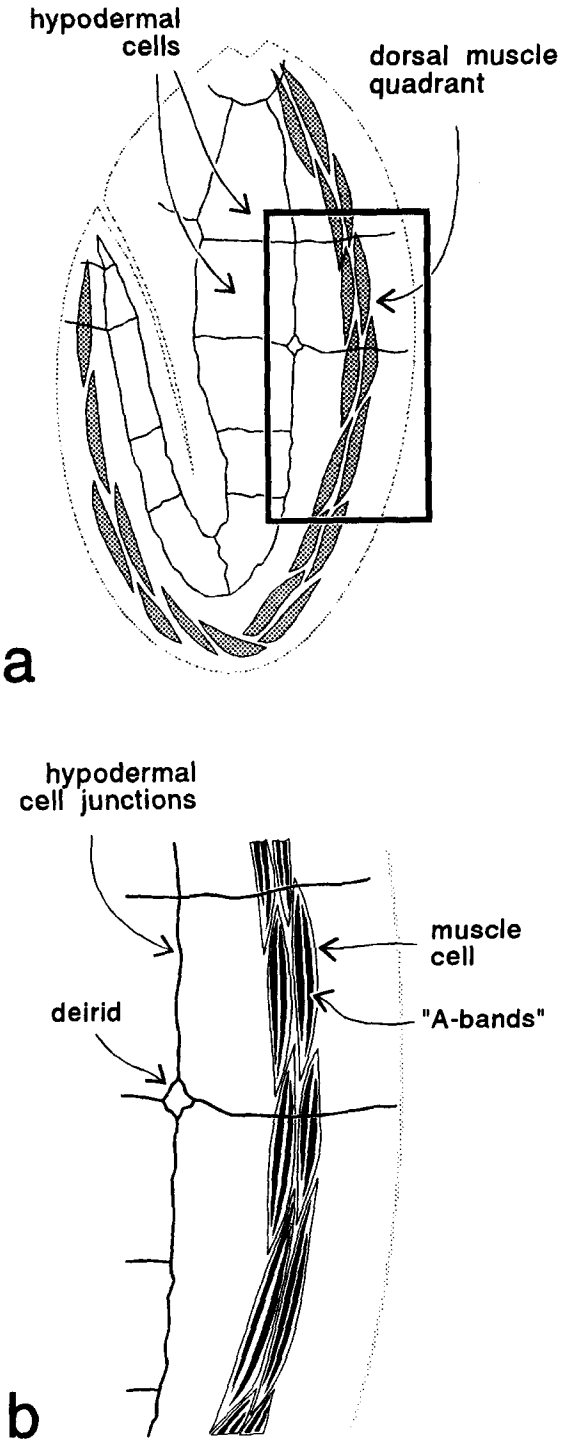

Figure 3. The arrangement of body wall muscle cells and hypodermal cells in a one-and-three-quarters-fold wild-type embryo. (*a*) Diagram of the left-dorsal surface of an embryo; the dorsal muscle quadrant is a double row of spindle-shaped cells (*shaded*) that are attached to the thin hypodermal cells covering the embryo. Boxed area approximates the region of mutant embryos shown in Fig. 5. (*b*) Detail of boxed region including the arrangement of myosin-containing A-bands within the muscle cells; note that there are four A-bands across the quadrant. Positions of hypodermal cell junctions are indicated, including the circular junction formed at the deirid sensillum. The monoclonal antibody MH27 recognizes the hypodermal cell junctions specifically.

A-bands per cell, so that four longitudinal bands of staining can be counted across the width of the quadrant (between arrows). In contrast, just 20 min earlier when embryos are at the one-and-one-quarter length and have not yet begun to move, mhcA is not yet organized into discrete A-bands and has a characteristic fibrous appearance (Fig. 4 *a*). The developmental sequence is described in more detail in the accompanying paper (Hresko et al., 1994). Note the position of the deirid (*arrowhead*, Fig. 4, *a* and *b*) in each embryo, and the changes in hypodermal cell shapes as the embryo lengthens.

Dorsal muscle quadrants of representative one-and-three-quarters-fold Pat mutants double stained with anti-mhcA and the antibody to hypodermal cell junctions are shown in Fig. 5 (area shown corresponds to box in Fig. 3 *a*). *myo-3* mutants are not shown because anti-mhcA staining is either absent or barely detectable (data not shown; Waterston, 1989).

The Pat genes can be divided into four classes based on mhcA organization in representative mutants. Class I, the most severely disorganized, includes *unc-52*, *unc-112*, *pat-3*, and *pat-2*. MhcA often appears as a single fibrous clump within each muscle cell (Fig. 5, *a–d*), leaving large gaps along the quadrant where staining is absent. These do not reflect gaps between the cells, however, since a polyclonal anti-myosin that also recognizes myosin heavy chain B (which has a more diffuse staining pattern) shows continuous staining along the quadrant, suggesting that cell shapes and positions are relatively normal (not shown). Since a significant amount of the mhcA staining in class I mutants is in a focal plane not associated with the hypodermal cells (not shown), it appears that mhcA has not been positioned normally at the sarcolemma adjacent to the hypodermis. We refer to this aspect of the phenotype as failure of the cells to polarize normally.

Class II genes include *pat-4*, *pat-6*, and *pat-11*. MhcA in the corresponding mutants is disorganized, but in contrast to the class I pattern, it stretches longitudinally within each cell so that there are fewer and shorter gaps in staining along the quadrant (Fig. 5, *f–h*). The staining appears in nearly the same focal plane as the hypodermal cells, suggesting proper cellular polarization. MhcA is not organized into A-bands, however.

Although *pat-2* is considered a class I gene based on the analysis of *pat-2 (st567)* (see above), another allele, *pat-2 (st538)*, results in a slightly less severe phenotype similar to the class II pattern (Fig. 5 *e*). This is the only case in which we have noted allele-specific differences in staining patterns.

Mutations in the class III (*pat-8*, *pat-9*, *pat-12*, and *deb-1*) and class IV (*lev-11*, *pat-5* and *pat-10*) genes allow mhcA to become partially organized into A-bands, indicated by three to four longitudinal lines of staining in each muscle quadrant (Fig. 5, *i–o*). The staining pattern of the class IV mutants appears to be better organized than that of the class III mutants, but neither is as well organized as the wild-type pattern (compare with Fig. 4 *b*). Class IV mutants are further distinguished from class III mutants by their actin organization in post-elongation-arrest embryos (see below).

The abnormal mhcA patterns seen in classes I, II, III, and IV are not simply the result of retarded muscle cell development. Each of these patterns is distinct from any seen in earlier wild-type embryos (compare with Fig. 4 *a*; data not shown).

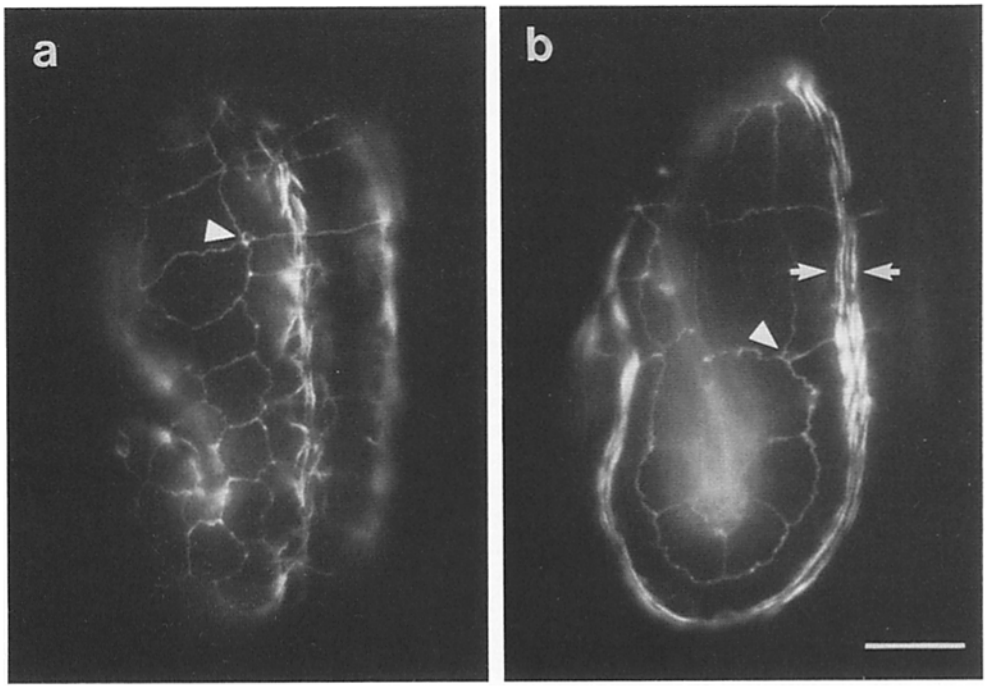

Figure 4. Wild-type embryos double stained with anti-mhcA and antibody MH27 which stains hypodermal cell junctions. MhcA is becoming organized into A-bands just as the first muscle contractions occur. (*a*) One-and-one-quarter-fold embryo (before first body wall muscle contractions); mhcA is becoming organized within the dorsal muscle quadrant in the plane of focus. MhcA staining has a characteristic fibrous appearance with some longitudinally oriented fibers suggesting that A-bands are beginning to form. (*b*) One-and-three-quarters-fold embryo (just after first muscle contractions); mhcA is organized into two discrete A-bands per cell, as indicated by the appearance of four longitudinal bands across the quadrant (*between arrows*). The position of the deirid sensillum (*arrowhead*), revealed by MH27 staining, is indicated in each embryo. Note the changes in hypodermal cell shape which occur as the embryo elongates. Bar, 10 μm.

Pat Embryos Stained with Anti-Actin

Actin organizes later than mhcA during wild-type development, often not forming distinct I-bands until after the three-fold stage (Hresko et al., 1994). Consequently, we were limited to comparing the actin staining of mutant embryos that were past the point of elongation arrest. Since we were not able to accurately stage the embryos by length, the individuals we examined may have been fixed at any time between elongation arrest and hatching. This introduces the possibility that abnormalities in the actin staining patterns may have been accentuated by continued abnormal muscle development, or reflect secondary deterioration of an originally well-organized pattern. Evidence of significant secondary deterioration was found for the two mild Pat mutants *pat-11(st541)* and *pat-12(st430)*, but not for the severe Pat mutants (see below). Typical mutants are shown in Fig. 6, and are arranged in the classes originally assigned through the mhcA staining; also included is a *myo-3* mutant (Fig. 6 *p*). Whole animals are shown and focal planes were chosen to include the best organized staining pattern within any of the four muscle quadrants.

Class I, II, and III mutants all showed a disorganized actin staining pattern. Class I mutants appeared to have diffuse staining within the muscle cells, while classes II and III often showed a fibrous, but still clearly disorganized pattern. The staining patterns for the two mild Pat mutants, *pat-11(st541)* and *pat-12(st430)*, should be considered the result of considerable post-arrest muscular deterioration, however (see below), so our data do not allow us to exclude the possibility that actin is initially well-organized in these two mutants.

In contrast to the mutants of classes I–III, those of class IV (Fig. 6, *m*, *n* and *o*), and the *myo-3* mutant (Fig. 6 *p*), have a relatively well-organized and continuous staining pattern that features thin longitudinal lines, suggesting the formation of I-bands.

There is relative agreement in the degree of mhcA and actin organization for mutants in classes I, II, and IV. In the Class III severe Pat mutants, however, mhcA appears better organized than actin, suggesting that the mutations preferentially affect the assembly of thin filaments into the myofilament lattice.

Conversely, *myo-3* mutants, which are unable to assemble normal thick filaments (Waterston, 1989), have a relatively well-organized actin-staining pattern (Fig. 6 *p*). No other Pat gene examined here is associated with mutations causing preferential disruption of thick filament organization into the lattice. Consequently, we have placed the *myo-3* gene in a phenotypic class by itself (class V).

Secondary displacements of dorsal muscle quadrants were observed in some post-arrest mutants, as has been reported previously for *myo-3* (Waterston, 1989) and *unc-45* (Venolia and Waterston, 1990) mutants. Examples can be seen in Fig. 6, *k*, *l*, and *p*; the dorsal muscle quadrants leave the outer (dorsal) curve of the embryo and are displaced ventrally in the region of the fold. Displacements were observed most frequently in *myo-3*, *lev-11*, *pat-5*, *pat-6*, *pat-8*, *pat-9*, *pat-10*, and *pat-12* mutants, and were not seen in one-and-three-quarters-fold animals.

Discontinuous Staining of Muscle Quadrants in Mild Pat and Lat Mutants Near the Time of Elongation Arrest

To address the possibility that the disorganized actin staining patterns seen in class I, II, and III post-elongation-arrest mu-

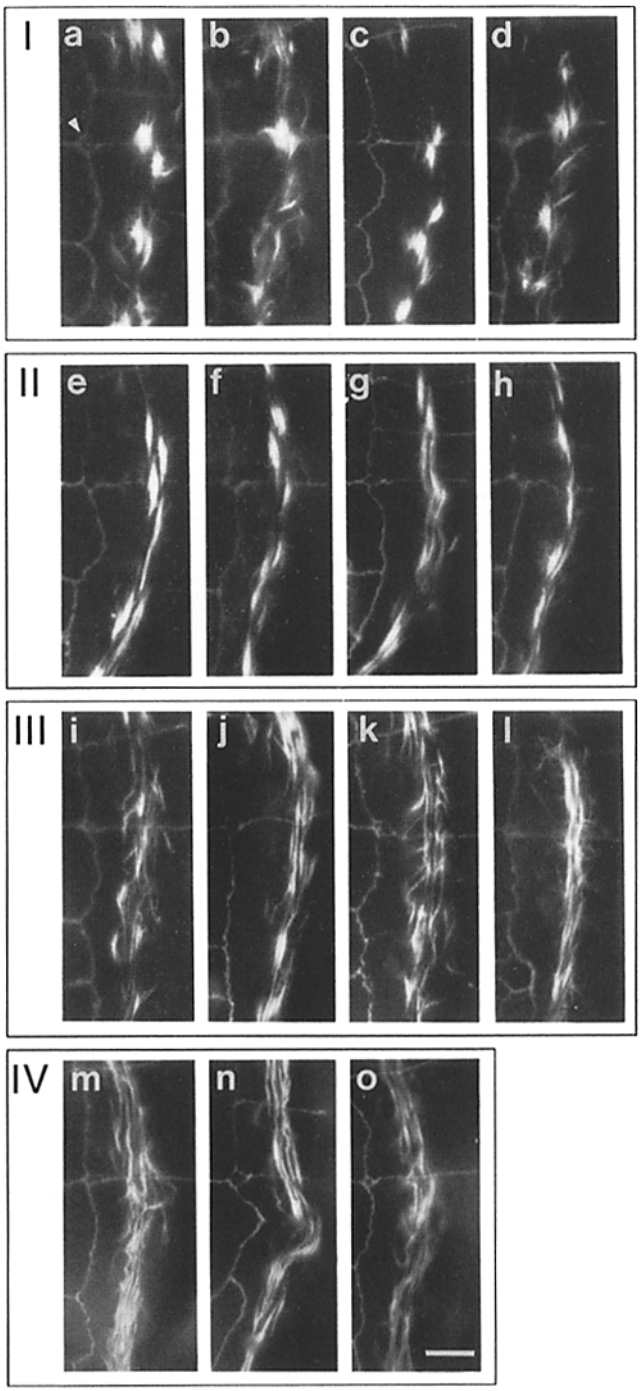

Figure 5. Representative one-and-three-quarters-fold Pat mutants double stained with a monoclonal antibody to mhcA and with an antibody to hypodermal cell junctions. The same part of a dorsal muscle quadrant is shown for each mutant, comparable to the boxed area in Fig. 3 *a*; note the deirid in each panel (see *arrowhead* in *a*). The embryos are divided into four classes, I–IV, each class with successively better mhcA organization. MhcA appears as a single unorganized clump in the muscle cells of class I mutants, leaving large gaps in the staining pattern within the muscle quadrant (*a–d*). In class II mutants (*e–h*) mhcA is slightly better organized, stretching longitudinally along the muscle quadrant, but does not appear to form normal A-bands. Class III mutants (*i–l*) have mhcA partially located in A-bands, as suggested by the three to four narrow longitudinal stripes of staining in the quadrant. MhcA in Class IV (*m–o*) mutants appears to be slightly better organized than in Class III mutants, but is not comparable to the wild-type pattern (compare to Fig. 4 *b*). Class IV mutants are also set apart from those of class III by their actin organization (see Fig. 6). Class I: (*a*) *unc-52(st549)*, (*b*) *unc-112(st562)*, (*c*) *pat-3(st552)*, and (*d*) *pat-2(st567)*. Class II: (*e*) *pat-2(st538)*, (*f*) *pat-4(st551)*, (*g*) *pat-6(st561)*, and (*h*) *pat-11(st541)*. Class III: (*i*) *deb-1(st385)*, (*j*) *pat-8(st554)*, (*k*) *pat-9(st558)*, and (*l*) *pat-12(st430)*. Class IV: (*m*) *lev-11(st557)*, (*n*) *pat-5(st556)*, and (*o*) *pat-10(st568)*. Bar, 5 μm.

tants are due to secondary degeneration of muscle, we assessed muscle deterioration by comparing anti-mhcA staining patterns of one-and-three-quarters-fold embryos with those of embryos fixed after elongation arrest. Although staining patterns in the post-arrest animals were no better organized than those seen in the younger animals, the patterns were comparable, with the exception of the two mild Pat mutants *pat-11* and *pat-12*. We identified discontinuities in mhcA staining along the muscle quadrants (Fig. 7, *a*, *b*, and *c*) of these mutants fixed during or soon after elongation arrest as judged by the undistorted shape of the embryos (the smooth shape of twofold arrest animals becomes progressively more distorted with time, as revealed by time-lapse observations). Similar discontinuities were not seen in wild-type or severe Pat embryos of similar age, nor in the mild Pat mutants at one-and-three-quarters-fold (not shown). Several hours after elongation arrest (as judged by distorted embryonic shape) each *pat-11* and *pat-12* embryo we observed had severely disorganized muscle, including discontinuities in quadrant staining (Fig. 7 *f*) and abnormal positioning of quadrants within the embryo (Fig. 7, *d* and *e*). Although it is difficult to interpret the nature of these discontinuities, they may reflect breaks in the muscle quadrants, perhaps due to detachment of muscle cells from the hypodermis. Consistent with this structural deterioration, time-lapse observations often show a shift from mild to more severe paralysis in *pat-11* and *pat-12* mutants contemporaneous with elongation arrest.

Since Lat mutants experience a dramatic loss of movement soon after they reach twofold length, we stained one of them, *emb-9(st540)*, with anti-mhcA to investigate its muscle structure. Although animals younger than twofold were indistinguishable from wild-type, some of the twofold animals fixed near the time of elongation arrest (as judged by their undistorted shapes), showed discontinuities in staining along their muscle quadrants (Fig. 8 *a*). All of the older arrested embryos, as judged by their distorted shapes, had a highly disorganized mhcA staining pattern featuring gaps in staining along the length of the muscle quadrants (Fig. 8 *b*). As with the mild Pat mutants, this phenotype may reflect breaks in the muscle quadrants due to local detachment of muscle cells from the hypodermis occurring soon after the animals reach the twofold stage.

Several Pat Mutants Fail to Stain with Antibodies to Specific Muscle Components

It has been shown previously that *myo-3* (Waterston, 1989), *deb-1* (Barstead and Waterston, 1991), and *unc-52* (Rogalski et al., 1993) Pat mutants fail to stain with antibodies to their corresponding gene products. These results suggest that in each case the mutation blocks the synthesis or accumulation of the affected protein. To help identify the gene products of

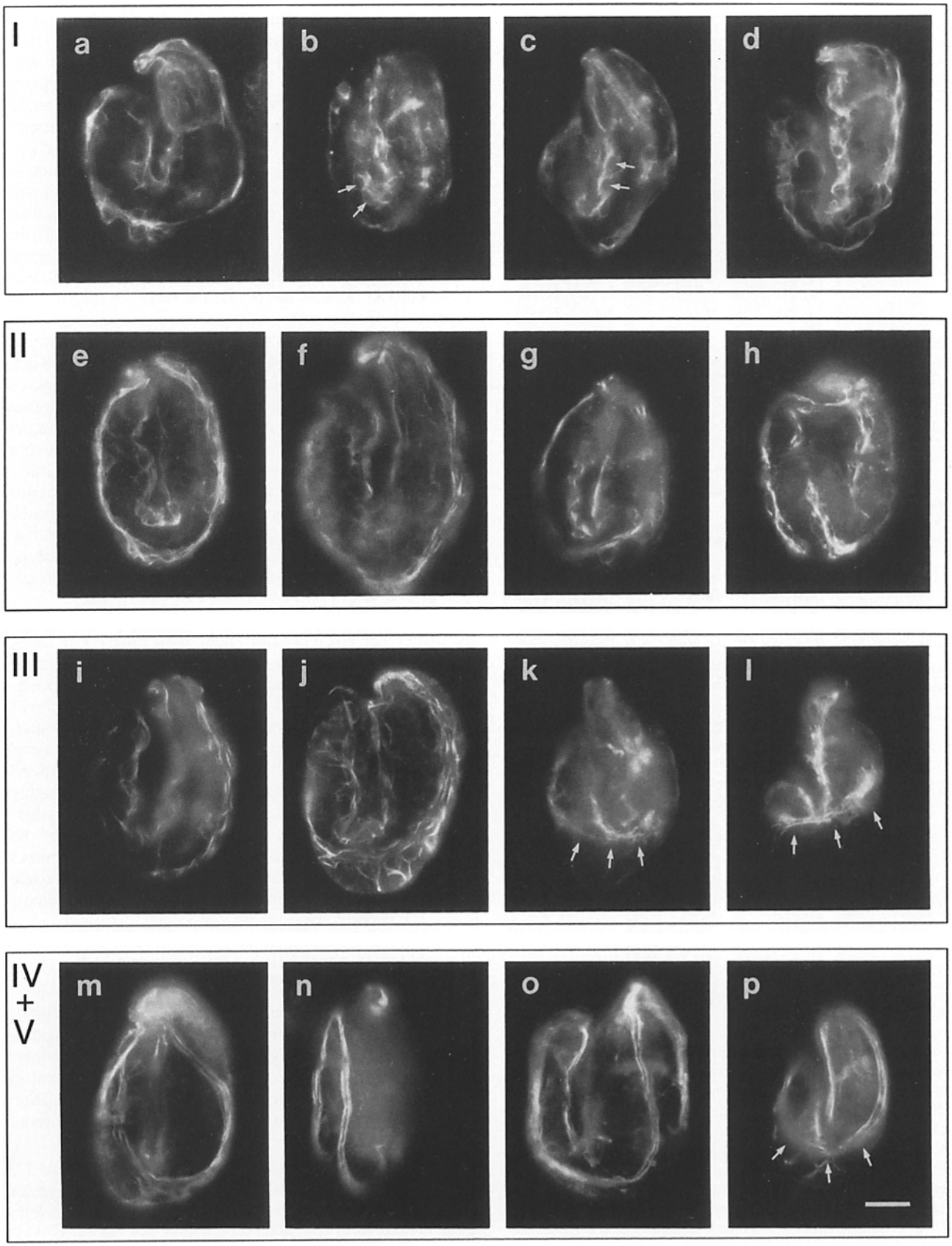

Figure 6. Representative Pat mutants after elongation arrest stained with a monoclonal antibody to actin. The plane of focus in each panel was chosen to show the best organized staining pattern within any of the four muscle quadrants. The mutants are arranged in classes I–IV as assigned through the anti-mhcA staining shown Fig. 5. In addition, a *myo-3* mutant, representing class V is shown (*p*). Class I mutants (*a–d*) have poorly organized actin which appears diffuse within the muscle cells and outlines the nuclei, which exclude the antigen (*c* and

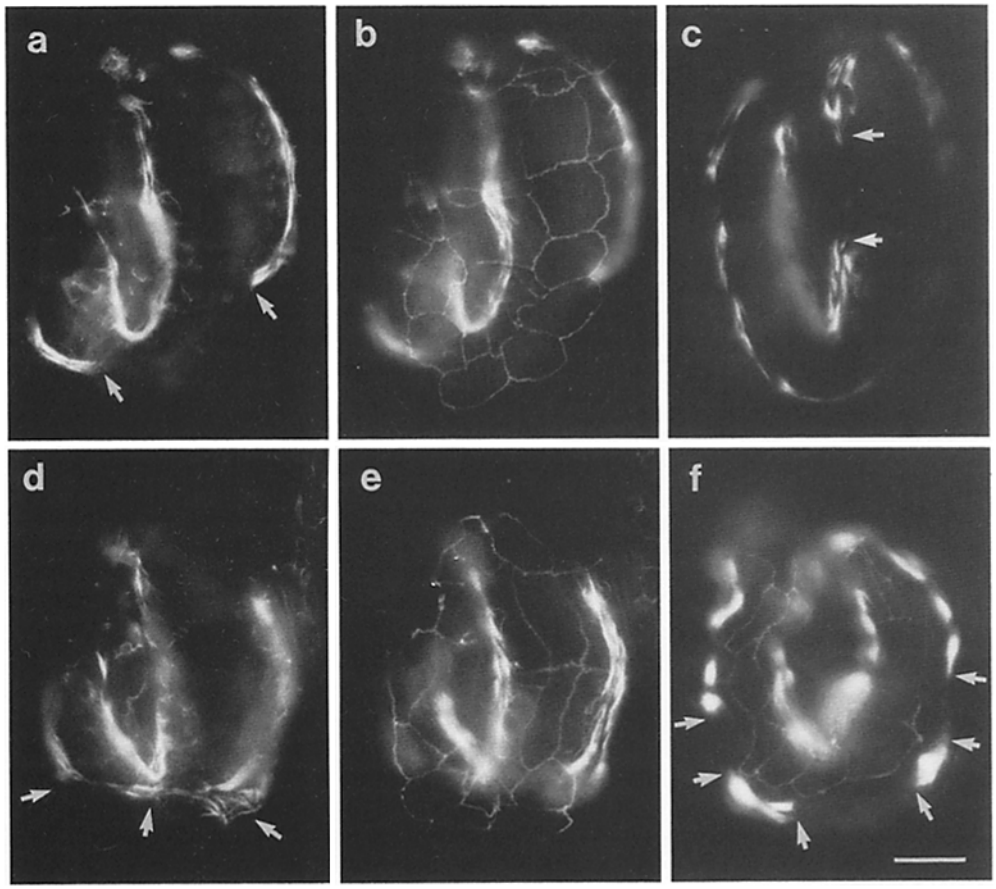

Figure 7. Mild Pat mutants develop discontinuities in staining along their muscle quadrants near the time of elongation arrest. Embryos were double stained with monoclonal antibodies to mhcA and to a component of hypodermal cell junctions. Embryos at the top (*a*, *b*, and *c*) were fixed during or soon after elongation arrest, as judged by their relatively normal shapes (see text). Embryos at the bottom (*d*, *e*, and *f*) were fixed later, as suggested by shape distortions characteristic of Pat mutants several hours after elongation arrest. *a* and *b*, two focal planes of a *pat-12(st430)* embryo selected to emphasize muscle cells and hypodermal cell junctions, respectively; *c*, *pat-11(st541)*. The discontinuous anti-mhcA staining along muscle quadrants (indicated by arrow pairs, *a* and *c*) suggest quadrant breaks, perhaps due to detachment of muscle cells from the hypodermis. The hypodermis is intact in the region of the gap in anti-mhcA staining in the *pat-12* embryo, as revealed by staining of hypodermal cell junctions (*b*). *d* and *e*, two focal planes of an older post-arrest *pat-12(st430)* embryo. A dorsal muscle quadrant fails to follow the outer curvature of the embryo (*d*, *arrows*), suggesting detachment from the hypodermis; hypodermal cell junctions in this embryo can be seen in *e*, *f*, older *pat-11(st541)* embryo; large gaps in staining along the muscle quadrants (indicated by *arrow pairs*) are similar to those seen in the younger post-arrest embryos (compare with *c*). Bar, 10 μm.

additional Pat genes, we have tested for the specific failure of several Pat mutants to stain with antibodies to other muscle components.

Staining of wild-type adult muscle with monoclonal antibodies MH2 and MH3 has shown that the *unc-52* gene product is concentrated within the basement membrane at positions where dense bodies (Z-line analogs) and M-lines are attached to the sarcolemma (Francis and Waterston, 1991). Since another antibody, MH25, appears to stain the sarcolemma at similar positions and has been speculated to bind an integrin (Francis and Waterston, 1985), we decided to test the class I mutants for staining with this antibody. Each of these mutants stained with MH25 (not shown), with the exception of the *pat-3* mutants, which were specifically negative (Fig. 9). Fig. 9 *a* shows a wild-type one-and-three-quarters-fold embryo double-stained with MH25, and with MH27, an antibody to hypodermal adherens junctions. MH25 stains a longitudinal strip corresponding to the position of each muscle quadrant (Fig. 9 *a*, *arrows*). In contrast, mutant *pat-3* animals have undetectable MH25 staining (Fig. 9 *b*, *open arrows*); the staining of hypodermal cell junctions by MH27 serves as a control for fixation of the embryo and penetration of the antibodies. These results suggest that *pat-3* may code for the MH25 antigen. Consistent with this possibility, *pat-3* has recently been shown to code for β-integrin by rescue of mutants with the wild-type gene (Gettner, S., C. Kenyon, L. Reichardt, J. Plenefisch, M. B. Buchner, and E. Hedgecock. 1992. *Mol. Biol. Cell.* 3:1088a).

lev-11 maps to a genetic interval containing the cloned tropomyosin gene (Kagawa, H., personal communication),

d, *arrows*). Class II (*e–h*) and Class III (*i–l*) mutants have actin staining that often appears fibrous, but is not well organized. Class IV mutants (*m–o*) and the *myo-3* mutant (*p*) have well-organized actin staining which appears continuous along the muscle quadrant and contains longitudinal stripes that suggest the organization of I-bands. In some post-arrest mutants, the dorsal muscle quadrants appear to be displaced from their normal position along the outer curve of the embryo, in the region of the fold (*arrows*, *k*, *l*, and *p*). Class I: (*a*) *unc-52(st572)*, (*b*) *unc-112(st562)*, (*c*) *pat-3(st552)*, and (*d*) *pat-2(st567)*. Class II: (*e*) *pat-2(st538)*, (*f*) *pat-4(st579)*, (*g*) *pat-6(st561)*, and (*h*) *pat-11(st541)*. Class III: (*i*) *deb-1(st385)*, (*j*) *pat-8(st554)*, (*k*) *pat-9(st558)*, and (*l*) *pat-12(st430)*. Class IV: (*m*) *lev-11(st536)*, (*n*) *pat-5(st569)*, and (*o*) *pat-10(st568)*. Class V: (*p*) *myo-3(st563)*. Bar, 10 μm.

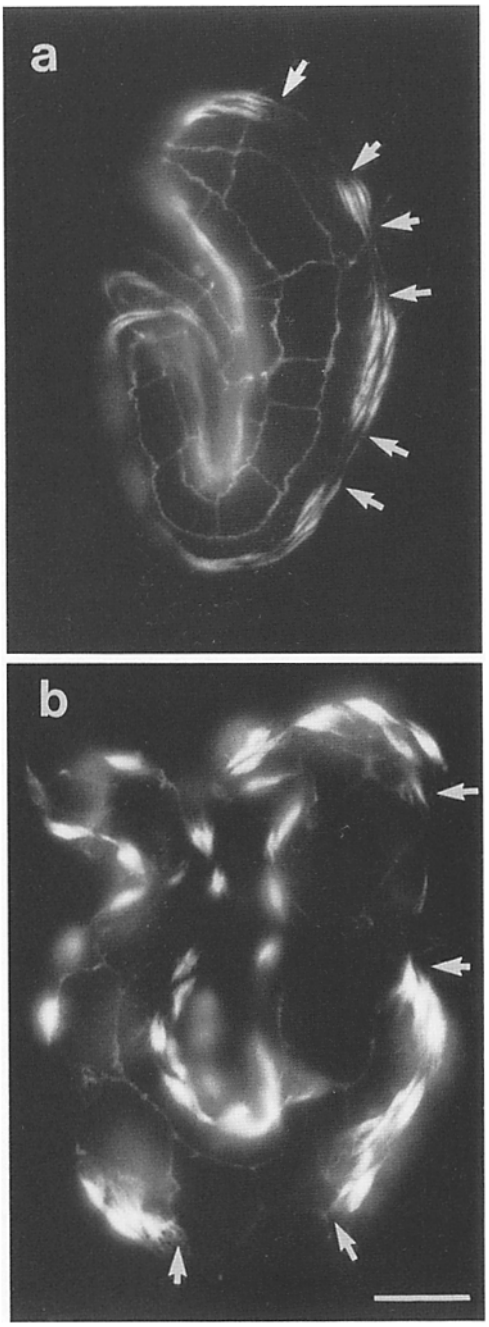

Figure 8. Development of discontinuities in staining of muscle quadrants in *emb-9(st540)* embryos near the time when animals become paralyzed and fail to continue elongation. Embryos were double stained with monoclonal antibodies to mhcA and to a component of hypodermal cell junctions. (*a*) Embryo fixed near the time of elongation arrest and onset of paralysis, as judged by its undistorted shape (see text). Well-organized A-bands, indistinguishable from wild-type (compare with Fig. 4 *b*), appear in parts of the muscle quadrant, but there are several areas along the quadrant which fail to stain (*between arrows*). These discontinuities may reflect breaks within the muscle quadrant correlating with the rapid onset of paralysis. (*b*) Embryo fixed several hours after elongation arrest, as judged by its distorted shape. Large gaps in the staining pattern along the muscle quadrants (*between arrows*) are similar to those observed in younger post-arrest embryos. MhcA does not appear in normal A-bands within these muscle cells. Bar, 10 μm.

as determined through correspondence between the genetic and physical *C. elegans* genome maps. Consequently, we decided to stain *lev-11* Pat mutants with affinity purified antitropomyosin antibodies raised against the *C. elegans* protein. Muscle cells of wild-type embryos stain with the antitropomyosin (Fig. 9 *c*, *arrows*), but the mutant embryos show greatly reduced or undetectable staining (Fig. 9 *d*, *open arrows*); again, staining of the hypodermal cell junctions serves as a positive control. These results provide indirect evidence consistent with the identification of *lev-11* as the tropomyosin gene. Ultimate proof must await transformation rescue of the mutants with the cloned gene and identification of sequence changes within the tropomyosin gene of *lev-11* mutants.

Discussion

The screen for Pat mutants has demonstrated the existence of a large class of muscle-affecting genes, each apparently essential for the formation of functional embryonic body wall muscles. The variety of muscle cell defects observed in the mutants and the identities of the gene products established to date suggest that there are several kinds of Pat genes. Some appear to be needed for myofilament lattice assembly, others specifically for the assembly of thin or thick filaments into the lattice, and several more for the regulation of contraction. Our analysis of several of the mutants provides direct evidence that the ECM and sarcolemma play critical roles in sarcomere formation, and is consistent with an assembly process starting at the membrane and proceeding into the cell. Future molecular analysis should identify more of the proteins involved, and analysis of mutant phenotypes should give additional insights into lattice assembly in vivo.

It seems unlikely that we saturated the class of severe Pat mutants, since only 6,800 haploid genomes have been screened, 5,800 in the screen reported here, and 1,000 in the previously reported unrestricted screen (Waterston, 1989). Genetic saturation would probably require a screen of at least 10,000 haploid genomes, assuming a forward mutation rate of 5×10^{-4} (Brenner, 1974) for each gene. Alternatively, we can gauge how close we are to saturation by estimating the total number of severe Pat genes by the frequency with which mutations were isolated for each of the genes. By assuming that the number of mutations per gene follows the Poisson distribution (considering only mutations recovered in the unrestricted screens), the estimated gene number is 13 (see Materials and Methods for details). This is certainly an underestimate since the calculation assumes that the probability for mutant recovery is the same for all genes; existence of genes with different probabilities for mutant recovery will cause the class size estimate to be too low. Nevertheless, since 13 severe Pat genes have been identified to date, the currently identified set probably represents a substantial fraction of the genes in the class.

Since the Pat mutations appear to have their primary effects on body wall muscle function and structure, it seems likely that the corresponding genes are expressed in these cells. This has been verified for *myo-3* (Waterston, 1989), and for *deb-1* (Francis and Waterston 1989; Barstead and Waterston, 1991) by the staining of muscle cells with anti-

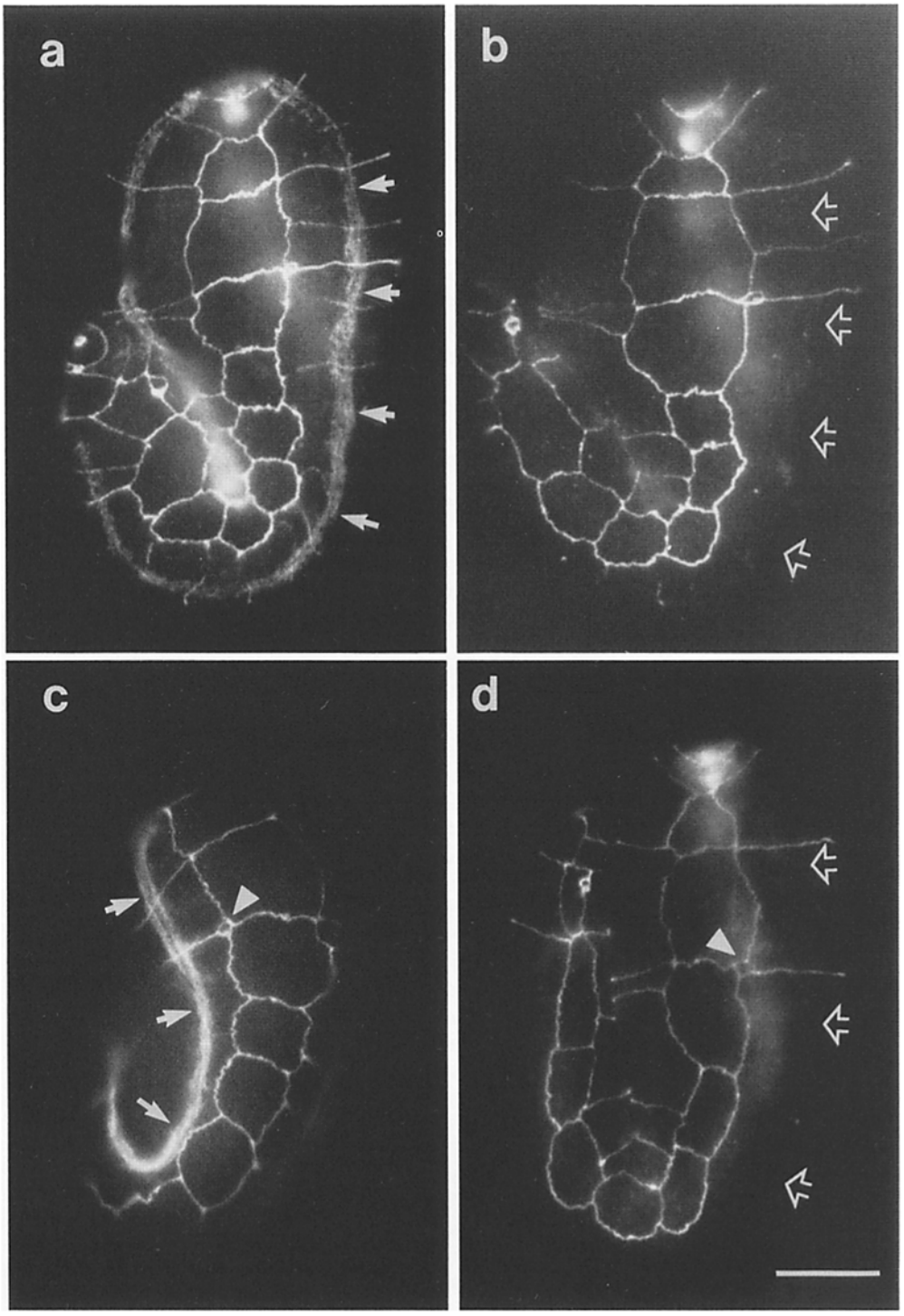

Figure 9. pat-3 and *lev-11* Pat mutants specifically fail to stain with antibodies recognizing a muscle cell membrane antigen and tropomyosin, respectively. (*a*) Wild-type and (*b*) pat-3(st552) mutant embryos stained with monoclonal antibody MH25 recognizing a muscle cell membrane antigen; hypodermal cell junctions are visualized in both embryos by staining with monoclonal antibody MH27. MH25 stains the dorsal muscle quadrant in the wild-type embryo (*a*, *arrows*), but fails to stain the *pat-3* mutant (*b*, *open arrows*). (*c*) Wild-type and (*d*) *lev-11(st557)* mutant embryos double stained with affinity-purified antibodies recognizing tropomyosin and with monoclonal antibody MH27. The anti-tropomyosin stains muscle cells of the wild-type embryo (*c*, *arrows*); the plane of focus includes a dorsal quadrant which is located on the inside bend because this embryo has rolled within the egg before fixation (note the position of the deirid in each embryo, *c* and *d*, *arrowheads*). The muscle cells of a comparable staged *lev-11* mutant fail to stain with the anti-tropomyosin antibody (*d*, *open arrows*). Bar, 10 μm.

bodies to the corresponding gene products. The *unc-52* gene product, which contributes to the basement membrane between muscle and hypodermal cells (Francis and Waterston, 1991; Rogalski et al., 1993) appears to be made by muscle and not by hypodermis based on staining of *zyg-1* mutant embryos. In these mutants, cytokinesis fails during early embryogenesis and separated clusters of cells expressing either muscle or hypodermal antigens can be identified; monoclonal antibodies MH2 and MH3, which stain the *unc-52* gene product, stain cell clusters expressing muscle antigens and not those expressing hypodermal antigens (Curry, A., G. R. Francis, and R. H. Waterston, unpublished results). The *pat-3* and *lev-11* genes also appear to be expressed in muscle cells based on staining of wild-type muscle cells with monoclonal antibody MH25 (Francis and Waterston, 1989) and anti-tropomyosin, respectively.

Since we concentrated our screen on mutants with little or no muscle function, we thought that some of them might

have defects in the genes controlling muscle cell determination and differentiation. These mutants might fail to express multiple antigens specific to differentiated muscle cells. Although we have identified many of the genes in the severe Pat class, none appear to be associated with this type of mutant phenotype. Failure to recover this type of mutant may reflect a partial redundancy in the genetic control of muscle cell differentiation, such that mutations in any single gene will fail to completely block differentiation. Indeed, mutants deficient for the *hlh-1* gene, which encodes the myoD homologue of *C. elegans*, express each of the several different muscle-specific antigens for which they were tested, but do have the mild Pat phenotype and abnormal muscle structure, both consistent with defects in muscle cell gene expression (Chen et al., 1992). Alternatively, genes controlling muscle cell determination and differentiation may also function in other types of cells. In this case, the corresponding mutants might have a phenotype other than severe Pat.

The effects on myofilament lattice assembly caused by mutations in the Pat genes are summarized in Table III. Of the genes with the most severe assembly defects (class I), *unc-52* and *pat-3* code for an ECM component homologous to vertebrate perlecan (Rogalski et al., 1993), and the membrane protein β-integrin (Gettner, S., C. Kenyon, L. Reichardt, J. Plenefisch, M. R. Buchner, and E. Hedgecock. 1992. *Mol. Biol. Cell.* 3:1088a), respectively, which have been colocalized to positions where dense bodies and M-lines are attached to the cell membrane (Francis and Waterston, 1985, 1991). The drastic effects on both thick and thin filament organization in the mutants suggest that myofilament lattice assembly may initiate at the cell membrane in steps involving these proteins. An alternate model that the lattice forms without significant participation of the membrane and is later anchored there, perhaps through the action of the *unc-52* and *pat-3* gene products, is inconsistent with our staining data since we failed to see even a partially organized lattice at any developmental stage in these mutants. The other class I genes, *unc-112* and *pat-2*, may encode other ECM or membrane components with similar critical roles in lattice assembly. Based on physical map data, an α-integrin gene discovered in the *C. elegans* genome sequencing project has been positioned near *pat-2* (Sulston et al., 1992; Waterston, R. H., personal communication). A *pat-2* mutant has been rescued with a cosmid from the physical genome map containing this gene as well as several other adjacent genes (our unpublished data). The possibility that *pat-2* codes for α-integrin deserves further investigation.

Table III. Pat Mutant Muscle Cell Phenotypes

Genes	Cell polarization	Myosin organization	Actin organization
Class I			
unc-52, unc-112, pat-2, pat-3	−	−	−
Class II			
*pat-4, pat-6, pat-11**	+	−	−
Class III			
*deb-1, pat-8, pat-9, pat-12**	+	+	−
Class IV			
lev-11, pat-5, pat-10	+	+	+
Class V			
myo-3	+	−	+

* Disorganized actin staining in *pat-11* and *pat-12* mutants may reflect secondary deterioration of body wall muscles occurring after elongation arrest (see text).

Direct evidence for involvement of the sarcolemma in myofilament lattice assembly has also come from analysis of the Drosophila mutant *myospheroid*, which has a defective β-integrin gene (MacKrell et al., 1988). These mutants appear to develop normally until the time of first muscular contractions. Subsequently, they exhibit a range of developmental abnormalities including defects in muscle attachment, structure, and function. In contrast to the muscle cells of *pat-3* mutants which never appear to contract based on our time-lapse analysis, the segmental and pharyngeal muscles of the myospheroid embryos initially contract, and then detach from their normal sites of attachment (Wright, 1960). Analysis of muscle cell structure in *myospheroid* mutants shows that although some early stages of myofilament lattice assembly appear to be normal (Newman and Wright, 1981), the lattice of older embryos is abnormal (Newman and Wright, 1981; Volk et al., 1990), consistent with a role for β-integrin in the maintenance of the myofilament lattice, and perhaps in its assembly. Consistent with the latter possibility, β-integrin-deficient muscle cells from *myospheroid* mutant embryos specifically fail to form Z-bands in culture (Volk et al., 1990).

Pat mutations which disrupt both thin and thick filament organization into the lattice, but allow polarized localization of mhcA at the appropriate cell membrane define the class II genes. The products of each of these genes are currently unknown.

Mutations in the class III genes appear to preferentially disrupt thin filament organization. Since *deb-1* codes for vinculin (Barstead and Waterston, 1989), which is a basal component of dense bodies, a preferential effect on thin filament organization might be expected, and has been reported previously (Barstead and Waterston, 1991). The similar defects in *pat-8* and *pat-9* mutants suggest that these genes may also code for proteins that contribute to dense bodies or are otherwise involved in the organization of thin filaments.

A partial independence in the assembly of thin and thick filaments into the lattice is suggested by the preferential disruption of thin filament organization seen in *deb-1, pat-8,* and *pat-9* mutants, and of thick filament organization in *myo-3* mutants. A similar independence was demonstrated previously in *Drosophila* mutants with indirect flight muscle cells deficient for either all sarcomeric actin or myosin isoforms; the former assembled A-band-like structures, and the latter, I-Z-I-like complexes (Beall, 1989). Assembly of thick filaments into sarcomere-like arrays in the absence of thin filaments has also been observed in vertebrate striated muscle cells treated with taxol in culture (Toyama et al., 1982).

Mutations in the class IV Pat genes do not have drastic effects on the assembly of either filament system, but do result in severe paralysis. The tentative identification of *lev-11* as the tropomyosin gene suggests that at least some of the genes of this class are involved in the regulation of muscle contraction. Interestingly, there is evidence that another class IV gene, *pat-10,* codes for a second component of the thin filament regulatory system, troponin C. The troponin C gene has been cloned (Kagawa, H., personal communication) and positioned using the physical map to a genetic interval containing *pat-10. pat-10* mutants have been rescued

by transformation with a yeast artificial chromosome clone from the physical map that contains the troponin C gene as well as other genes in the region (our unpublished results); identification of *pat-10* as the troponin C gene will require rescue with DNA fragments that contain only the troponin C gene, however. The only other class IV gene, *pat-5*, may be an unusually large genetic target, based on the many mutants recovered at this locus.

The appearance of discontinuities within muscle quadrants is a distinctive feature that the mild Pat mutants *pat-11* and *pat-12* share with the type IV collagen mutant *emb-9*, and may be the result of failing muscle-hypodermal attachments. Since type IV collagen is found exclusively in basement membranes and is a major component of these specialized extracellular matrices (Glanville, 1987), defects in the basement membrane between the muscle and hypodermal cells may be responsible for weakened attachments in the *emb-9* mutants. Based on the phenotypic similarity, it could be argued that *pat-11* and *pat-12* code for components directly involved in attaching muscle cells to the hypodermis. Since, in contrast to the *emb-9* mutant, partial paralysis and abnormalities in myofilament lattice structure precede the appearance of discontinuities in the muscle quadrants, *pat-11* and *pat-12* may affect components within the muscle cell involved in anchoring it to the hypodermis and also necessary for normal lattice assembly. Alternatively, any effects on muscle cell attachment may simply be indirect consequences of failure to form a normal lattice. In any case, the preliminary characterization of these mild Pat mutants, and the fact that *unc-45* mutants (Venolia and Waterston, 1990) and *hlh-1* deficient animals (Chen et al., 1992) have the mild Pat phenotype, suggests that analysis of mild Pat mutants obtained in large scale screens are likely to identify other critical muscle-affecting genes.

Although *emb-9* and *unc-52* each appear to code for basement membrane components, it is noteworthy that mutations in these genes have very different effects on myofilament lattice assembly. Assembly starts normally and proceeds relatively far in the *emb-9* mutants (Fig. 8 *a*), but is obviously disrupted at a very early stage in the *unc-52* mutants (Fig. 5 *a*). As discussed above, perlecan, the *unc-52* gene product (Rogalski et al., 1993), appears to play a critical role in early lattice assembly. In contrast, the $\alpha 2$ subunit of type IV collagen, the *emb-9* gene product (Sibley et al., 1993), appears to be dispensable for early lattice assembly, but involved in the maintenance of cell attachments, perhaps through bolstering the structural integrity of the basement membrane.

Embryonic elongation appears to be the result of forces generated by the cytoskeleton within the hypodermal cells, which squeeze the embryo forcing it to change shape (Priess and Hirsh, 1986). It has been argued previously for *myo-3* (Waterston, 1989) and *deb-1* (Barstead and Waterston, 1991) Pat mutants that failure to complete elongation may be a secondary consequence of a failed interaction between muscle and hypodermal cells, rather than a primary defect in the hypodermal cells themselves. Many of the Pat mutants isolated here appear to have primary defects in body wall muscle cells, consistent with this hypothesis. Time-lapse analysis shows that elongation failure in the *emb-9* and *let-2* mutants is tightly correlated with a rapid onset of paralysis, providing further evidence that functioning muscle is necessary for elongation to proceed past the twofold length.

One of the exciting implications of the results reported here, aside from the identification of many new genes critical for muscle cell function, is that further characterization of the Pat mutants should provide new information about myofilament lattice assembly. For instance, antibodies have helped partially define a chain of molecules that starts with the ECM, moves through the cell membrane and the dense body, and then ends with the thin filaments in the myofilament lattice (Francis and Waterston, 1985, 1991). The limited characterization of Pat mutants with anti-myosin and anti-actin antibodies presented here is consistent with an assembly process starting at the cell membrane, and perhaps continuing with the step-wise addition of components to form structures like the dense body. Antibody staining of wild-type embryos at different stages of lattice assembly provides further evidence for this idea (Hresko et al., 1994). The Pat mutants, in combination with the collection of antibodies, now offer an opportunity to directly test some of the predictions of this assembly model. Toward this end we have started to use antibody staining to investigate the assembly states of various muscle components in Pat mutants that are missing specific ECM, membrane, and internal cell proteins. The results of this analysis are presented in the accompanying paper (Hresko et al., 1994).

We thank R. Barstead, T. Schedl, and the members of the Waterston laboratory for many helpful discussions. We also thank J. Waddle for performing the deficiency mapping of *deb-1*, *pat-8*, and *unc-82*, M. C. Hresko and L. Schriefer for gift of anti-tropomyosin antibodies, D. Miller for gift of monoclonal antibody DM5.6, J. Plenefisch for some of the strains used in mapping, T. Schedl for suggesting the complementation test method using *tra-2(q122)*, and R. J. Lye for comments on the manuscript.

This work was supported by National Institutes of Health grants GM23883 to R. H. Waterston and postdoctoral fellowship GM12625 to B. D. Williams. Some of the strains used in this work were supplied by the *Caenorhabditis* Genetics Center, which is funded by the National Institutes of Health National Center for Research Resources.

References

Ardizzi, J. P., and H. F. Epstein. 1987. Immunological localization of myosin heavy chain isoforms and paramyosin in developmentally and structurally diverse muscle cell type of the nematode *Caenorhabditis elegans*. *J. Cell Biol.* 105:2763–2770.

Beall, C. J., M. A. Sepanski, and E. A. Fyrberg. 1989. Genetic dissection of *Drosophila* myofibril formation: effects of actin and myosin heavy chain null mutations. *Genes & Dev.* 3:131–140.

Barstead, R. J., and R. H. Waterston. 1989. The basal component of the nematode dense-body is vinculin. *J. Biol. Chem.* 264:10177–10185.

Barstead, R. J., and R. H. Waterston. 1991. Vinculin is essential for muscle function in the nematode. *J. Cell Biol.* 114:715–724.

Barstead, R. J., L. Kleiman, and R. H. Waterston. 1991. Cloning, sequencing and mapping of an α-actinin gene from the nematode *Caenorhabditis elegans*. *Cell Motil. Cytoskeleton.* 20:69–78.

Brenner, S. 1974. The genetics of *Caenorhabditis elegans*. *Genetics.* 77:71–94.

Casella, J. F., S. W. Craig, D. J. Maack, and A. E. Brown. 1987. Cap Z, a barbed end actin-capping protein, is a component of the Z-line of skeletal muscle. *J. Cell Biol.* 105:371–379.

Chen, L., M. Krause, B. Draper, H. Weintraub, and A. Fire. 1992. Body-wall muscle formation in *Caenorhabditis elegans* embryos that lack the MyoD homolog *hlh-1*. *Science (Wash. DC).* 256:240–243.

Cummins, C., and P. Anderson. 1988. Regulatory myosin light-chain genes of *Caenorhabditis elegans*. *Mol. Cell Biol.* 8:5339–5349.

Epstein, H. F., R. H. Waterston, and S. Brenner. 1974. A mutant affecting the heavy chain of myosin in *Caenorhabditis elegans*. *J. Mol. Biol.* 90:291–300.

Francis, G. R., and R. H. Waterston. 1985. Muscle organization in *Caenorhabditis elegans*: localization of proteins implicated in thin filament attachment and I-band organization. *J. Cell Biol.* 101:1532–1549.

Francis, R., and R. H. Waterston. 1991. Muscle cell attachment in *Caenorhabditis elegans*. *J. Cell Biol.* 114:465–479.

Glanville, R. W. 1987. Type IV collagen. *In* Structure and Function of Collagen Types. Mayne, R., and R. E. Burgeson, editors. Academic Press, Orlando,

FL. 43–79.
Guo, X., J. J. Johnson, and J. M. Kramer. 1991. Embryonic lethality caused by mutations in basement membrane collagen of *C. elegans*. *Nature (Lond.)*. 349:707–709.
Hresko, M. C., B. D. Williams, and R. H. Waterston. 1994. Assembly of body wall muscle and muscle cell attachment structures in *Caenorhabditis elegans*. *J. Cell Biol.* In press.
Lewis, J. A., C.-H. Wu, H. Berg, and J. H. Levine. 1980. The genetics of levamisole resistance in the nematode *Caenorhabditis elegans*. *Genetics*. 95:905–928.
MacKrell, A. J., B. Blumberg, S. R. Haynes, and J. H. Fessler. 1988. The lethal myospheroid gene of Drosophila encodes a membrane protein homologous to vertebrate integrin β subunits. *Proc. Natl. Acad. Sci. USA*. 85: 2633–2637.
Meneely, P. M., and R. K. Herman. 1979. Lethals, steriles and deficiencies in a region of the *X* chromosome of *Caenorhabditis elegans*. *Genetics*. 92:99–115.
Miller, D. M., I. Ortiz, G. C. Berliner, and H. F. Epstein. 1983. Differential localization of two myosins within nematode thick filaments. *Cell*. 34: 477–490.
Miwa, J., E. Schierenberg, S. Miwa, and G. Von Ehrenstein. 1980. Genetics and mode of expression of temperature sensitive mutations arresting embryonic development in *Caenorhabditis elegans*. *Dev. Biol.* 76:160–174.
Newman, S. M., and T. R. F. Wright. 1981. A histological and ultrastructural analysis of the development defects produced by the mutation *lethal(1) myospheroid* in *Drosophila melanogaster*. *Dev. Biol.* 86:393–402.
Priess, J. R., and D. I. Hirsh. 1986. *Caenorhabditis elegans* morphogenesis: the role of the cytoskeleton in elongation of the embryo. *Dev. Biol.* 117:156–173.
Rogalski, T. M., B. D. Williams, G. P. Mullen, and D. G. Moerman. 1993. Products of the *unc-52* gene in *Caenorhabditis elegans* are homologous to the core protein of the mammalian basement membrane haparan sulfate proteoglycan. *Genes & Dev.* 7:1471–1484.
Sibley, M. H., J. J. Johnson, C. C. Mello, and J. M. Kramer. 1993. Genetic identification, sequence, and alternative splicing of the *Caenorhabditis elegans* α2(IV) collagen gene. *J. Cell Biol.* 123:255–264.
Sulston, J., and J. Hodgkin. 1988. Methods. *In* The Nematode *Caenorhabditis elegans*. W. B. Wood, editor. Cold Spring Harbor Laboratory, Cold Spring Harbor, New York. 587–606.
Sulston, J. E., E. Schierenberg, J. G. White, and J. N. Thomson. 1983. The embryonic cell lineage of the nematode *Caenorhabditis elegans*. *Dev. Biol.* 100:64–119.
Sulston, J., Z. Du, K. Thomas, R. Wilson, L. Hillier, R. Staden, N. Halloran, P. Green, J. Thierry-Mieg, L. Qui, S. Dear, A. Coulson, M. Craxton, R. Durbin, M. Berks, M. Metzstein, T. Hawkins, R. Ainscough, and R. Waterston. 1992. The *C. elegans* genome sequencing project: a beginning. *Nature (Lond.)*. 356:37–41.
Toyama, Y., S. Forry-Schaudies, B. Hoffman, and H. Holtzer. 1982. Effects of taxol and colcemid on myofibrillogenesis. *Proc. Natl. Acad. Sci. USA*. 79:6556–6560.
Venolia, L., and R. H. Waterston. 1990. The *unc-45* gene of *Caenorhabditis elegans* is an essential muscle-affecting gene with maternal expression. *Genetics*. 126:345–353.
Volk, T., L. I. Fessler, and J. H. Fessler. 1990. A role for integrin in the formation of sarcomeric cytoarchitecture. *Cell*. 63:525–536.
Waddle, J. A., J. A. Cooper, and R. H. Waterston. 1993. The α and β subunits of nematode actin capping protein function in yeast. *Mol. Biol. Cell*. 4:907–917.
Waterston, R. H. 1988. Muscle. *In* The Nematode *Caenorhabditis elegans*. W. B. Wood, editor. Cold Spring Harbor Laboratory, Cold Spring Harbor, New York. 281–335.
Waterston, R. H. 1989. The minor myosin heavy-chain, MHC A, of *Caenorhabditis elegans* is necessary for the initiation of thick filament assembly. *EMBO (Eur. Mol. Biol. Organ.) J.* 8:3429–3436.
Waterston, R. H., D. Hirsh, and T. R. Lane. 1984. Dominant mutations affecting muscle structure in *Caenorhabditis elegans* that map near the actin gene cluster. *J. Mol. Biol.* 180:473–496.
Waterston, R. H., D. G. Moerman, D. L. Baillie, and R. R. Lane. 1982. Mutations affecting myosin heavy chain accumulation and function in the nematode *Caenorhabditis elegans*. *In* Disorders of the Motor Unit. D. M. Schotland, editor. John Wiley, New York. 747–760.
Waterston, R. H., J. N. Thomson, and S. Brenner. 1980. Mutants with altered muscle structure in *Caenorhabditis elegans*. *Dev. Biol.* 77:271–302.
Williams, B. D., B. Schrank, C. Huynh, R. Shownkeen, and R. H. Waterston. 1992. A genetic mapping system in *Caenorhabditis elegans* based on polymorphic sequence-tagged sites. *Genetics*. 131:609–624.
Wright, T. F. 1960. The phenogenetics of the embryonic mutant, *lethal myospheroid*, in *Drosophila melanogaster*. *J. Exp. Zool.* 143:77–99.